

Simplified Method to Estimate the Green–Ampt Wetting Front Suction and Soil Sorptivity with the Philip–Dunne Falling-Head Permeameter

C. M. Regalado,* A. Ritter, J. Álvarez-Benedí, and R. Muñoz-Carpena

ABSTRACT

Wetting front suction and soil sorptivity (S) are relevant parameters to water movement in the vadose zone. Both may be estimated with the Philip–Dunne falling-head permeameter, given the moisture increment ($\Delta\theta$) and measured times (t_{med} and t_{max}) during an infiltration event. Previous studies have shown that the Philip–Dunne falling head permeameter can be used for estimating saturated hydraulic conductivity (K_s), but its potential to estimate the soil's sorptivity has received little attention. We investigate the ability of the Philip–Dunne method to estimate S and the Green–Ampt's suction at the wetting front, Ψ , by performing a parameter sensitivity analysis, focusing on the boundary conditions that limit the search space of physically sound solutions, and studying the shape factors used in Philip's analysis to reduce the three-dimensional flux of water in the soil to one dimension. Finally, a useful approximate solution is provided that allows computing both K_s and the Green–Ampt's suction at the wetting front, Ψ , (and hence the macroscopic capillary length parameter, α^*) from only two infiltration times, t_{med} and t_{max} , without having to resort to such a costly measurement as the soil moisture increment, $\Delta\theta$, required by the original method.

IN 1993 JOHN PHILIP, motivated by infiltration data provided by T. Dunne and E. Safran after a scientific campaign in the Amazon basin, published the Green–Ampt approximate analysis to estimate the saturated hydraulic conductivity (K_s) from the time course of water depth of a lined tube tightly inserted into a borehole (Philip, 1993). Later, De Haro et al. (1998) investigated the utility and applicability conditions of Philip's method by studying the sensitivity of the K_s estimation to the tube's initial height (h_0), the downward infiltration times when the permeameter is half full (t_{med}) and empty (t_{max}), and the increment in soil water content ($\Delta\theta$) after an infiltration experiment. Gómez et al. (2001) compared the Philip–Dunne falling-head permeameter with the ring, tension infiltrometer, and rainfall simulator, finding similar results for the estimated K_s , but not for the wetting front suction, Ψ (m). These authors could not give a definitive explanation to justify the high Ψ values obtained with the falling head permeameter. Muñoz-Carpena et al. (2002) also obtained large Ψ and K_s values when they compared the Philip–Dunne and constant head well permeameters; they explained the large values in terms of repre-

sentative elementary volume, soil anisotropy, and infiltration geometry differences between both methods. In an attempt to improve the field applicability of the Philip–Dunne permeameter, García-Sinovas et al. (2001) designed a prototype for automatic reading of the time course of water depth, confirming the results obtained by Muñoz-Carpena et al. (2002) in soils with different textures.

Most field techniques estimate K_s and Ψ under steady-state constant head conditions. However, insufficient information is obtained from the steady-state outflow rate under a single constant head to evaluate both K_s and Ψ , and thus multiple-head approaches or a site-estimated or independent measurement of Ψ are necessary. Multiple-, constant-head techniques may render physically unrealistic negative K_s values, because of soil profile discontinuities (Elrick and Reynolds, 1992) and ill-conditioning of equations (Philip, 1985). By contrast, the single-, constant-head analysis provides only a direct measure of K_s . Measurements under falling-head conditions have thus been proposed as an alternative to constant-head experiments. Falling-head techniques have the advantage of requiring smaller measurement times, and thus are preferred for measuring K_s in low infiltrating soils, which may require up to several hours to reach steady state with the constant-head methods.

Soil sorptivity, S ($\text{m s}^{-1/2}$), can be computed from $S^2 \approx 2K_s\Psi\Delta\theta$ (Philip, 1969), assuming a Green–Ampt infiltration wetting front and given the values of K_s , Ψ , and soil moisture increment, $\Delta\theta = \theta_s - \theta_0$, where θ_s ($\text{m}^3 \text{m}^{-3}$) is the field-saturated volumetric soil water content, and θ_0 is the initial or antecedent background volumetric soil moisture at the time of the measurement. The soil sorptivity characterizes the early stage of zero-ponded water infiltration, and thus represents the effect of the soil's matric potential. Consequently, both K_s and S are needed to characterize zero-ponded water infiltration into unsaturated soil, as proposed by Philip (1987):

$$I(t) = \frac{1}{2}St^{-1/2} + A \quad [1]$$

where I (m s^{-1}) is infiltration rate, t is time, and A is found to range from $0.33K_s$ to K_s (Youngs, 1964). In Eq. [1], the weight of the capillarity (sorptivity) decreases with the square root of t , while the last term in Eq. [1] is time independent, and thus reflects the maximum value of infiltration rate, such that as $t \rightarrow \infty$, $I = A$. Other hydraulic properties can be computed from the K_s and S estimates, including the macroscopic capillary length parameter, α^* (White and Sully, 1987), soil diffusivity (Brutsaert, 1979), and the unsaturated hydraulic conductivity curve (Gardner, 1958).

The Philip–Dunne falling head permeameter has received limited testing recently. Previous studies have

C.M. Regalado and A. Ritter, Instituto Canario Investigaciones Agrarias (ICIA), Dep. Suelos y Riegos, Apdo. 60 La Laguna, 38200 La Laguna, Spain; J. Álvarez-Benedí, Instituto Tecnológico Agrario de Castilla y León, Apdo. 172, 47080 Valladolid, Spain; R. Muñoz-Carpena, Agricultural and Biological Engineering Dep., University of Florida, 101 Frazier Rogers Hall, P.O. Box 110570, Gainesville, FL 32611-0570. Received 5 July 2004. Special Section: ZNS'03 Vadose Zone Research. *Corresponding author (cregalad@icia.es).

Published in Vadose Zone Journal 4:291–299 (2005).

doi:10.2136/vzj2004.0103

© Soil Science Society of America

677 S. Segoe Rd., Madison, WI 53711 USA

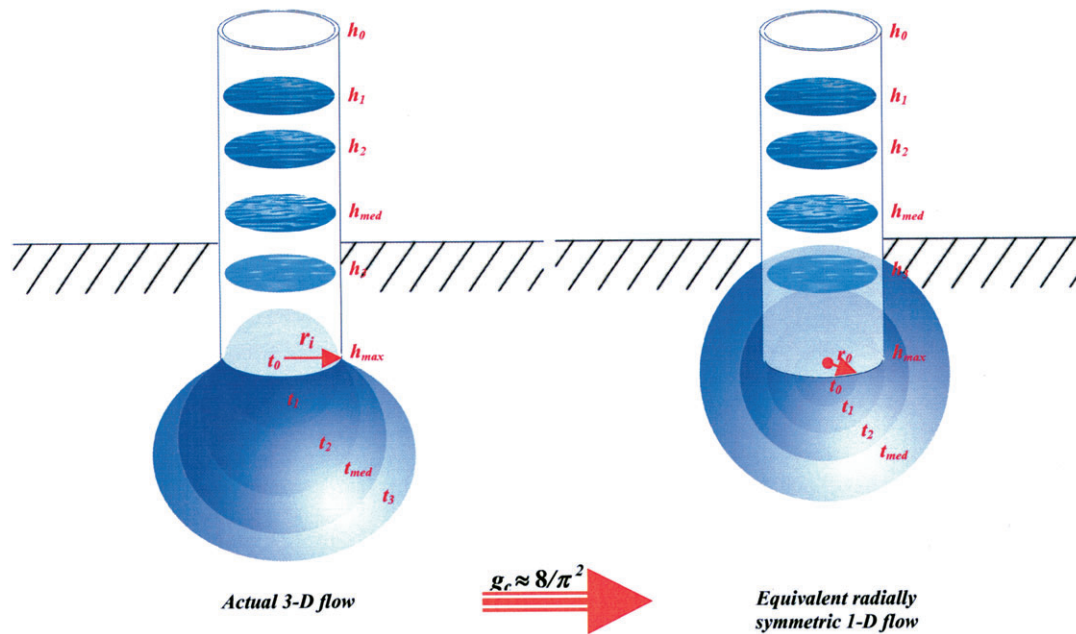


Fig. 1. Geometrical analog of the Philip–Dunne falling-head permeameter.

concentrated their efforts on showing experimentally the utility of Philip's falling-head permeameter for measuring K_s , while the estimation of the soil sorptivity received almost no attention. Alternative methods to measure soil sorptivity are the constant-head well permeameter, tension infiltrometer, measurement of infiltration using multiple discs with different radii, or single discs at various supply potentials (Minasny and McBratney, 2000). In this work we investigated the ability of the Philip–Dunne method to estimate Ψ and S , analyzing the boundary conditions that limit the search space of physically sound solutions, and the shape factors used in Philip's analysis to reduce to one dimension the three-dimensional flux of water in the soil. Also a sensitivity analysis of the method is performed. Finally, a useful approximate solution is provided that permits computing both K_s and the Green–Ampt suction at the wetting front, Ψ (and hence the macroscopic capillary length parameter, α^*), from only two infiltration times, t_{med} and t_{max} , without the need to measure the soil moisture increment, $\Delta\theta$, which is generally costly in terms of time and equipment (Muñoz-Carpena et al., 2002).

THEORY

The Philip–Dunne falling head permeameter consists of an open-ended tube of internal radius, r_i , which is inserted to the bottom of a borehole augered into unsaturated soil. The seal between the tube and borehole wall must be water-tight. At $t = t_0$, the tube is rapidly filled to height, $h = h_0$, and the fall of water level with time is monitored (Fig. 1). Philip's (1993) analysis of the flow out of the tube and into the soil begins with a geometrical simplification: the actual infiltration surface (a wetted disk that evolves toward a quasi-spherical bulb) is substituted by a sphere of equivalent surface area (i.e., with radius $r_o = r_i/2$). The flow is primarily pressure-

capillarity driven and it is perturbed by superposing on it, symmetrically, the gravitational component (Philip, 1993). The resulting equivalent flux is approximated to the actual flux by a geometrical coefficient $g_c = 8/\pi^2$ (Fig. 1). This assumption simplifies the description of the actual three-dimensional flow of water in the soil to a single radial coordinate r . The flow may be considered three-dimensional when a wetting volume, V_m , equivalent to a cylinder of radius r_i and height $2r_i$ is achieved (i.e., $V_m = 2\pi r_i^3 = 16\pi r_o^3$) or, in terms of the permeameter's height, when $h_0 - h = 4\Delta\theta r_o$. Preliminary computations showed that in our case, with $r_i = 0.018$ m and $h_0 = 0.3$ m, this volume is achieved when $h_0 - h(t) = 0.24$ m. Hence, the following approximate Green–Ampt analysis, based on the “effective hemisphere model” for trickle source unsteady infiltration, can be considered valid in such cases for time periods longer than the time required for the water level to fall 0.06 m. Details of the mathematical analysis may be found in Philip (1993). We develop next only those concepts that will be necessary to follow the work presented here.

From the mass conservation principle, the following relation between the pipe's water level $h(t)$ and the wetting (spherical) bulb radius $R(t)$ may be written as

$$h(t) = h_0 - \frac{1}{3} \Delta\theta \left[\frac{R(t)^3}{r_o^2} - r_o \right] \quad [2]$$

Differentiation of the previous expression leads to

$$\frac{dh}{dt} = -\Delta\theta \left(\frac{R}{r_o} \right)^2 \frac{dR}{dt} \quad [3]$$

Thus we arrive at the following differential equation by eliminating dR/dt from Eq. [3] (see Philip (1993) for details):

Table 1. Physicochemical properties (mean ± standard deviation) of soil samples used in this study.†

Soil	Classification	ρ_b kg m ⁻³	pH	OM	θ		Textural class
					θ_{33}	θ_{1500}	
1	Andisol	940 ± 60	7.0 ± 0.40	2.33 ± 0.55	38.3 ± 7.6	28.7 ± 3.4	L-C
2	Xerofluvents	1570 ± 120	7.9 ± 0.15	1.60 ± 0.21	11.9 ± 0.3	5.7 ± 0.1	L-S
3	Xerorthent	1300 ± 70	8.3 ± 0.20	0.85 ± 0.33	39.0 ± 1.9	22.2 ± 2.3	L-C
4	Xerocrept	1460 ± 60	6.9 ± 0.10	0.55 ± 0.03	4.9 ± 0.6	2.0 ± 0.3	L-S
5	Xerofluvents	1280 ± 60	8.6 ± 0.02	0.66 ± 0.07	16.5 ± 0.5	6.3 ± 0.2	L-C
6	Fulvudand	640 ± 110	5.0 ± 0.33	16.3 ± 8.0	34.7 ± 9.3	25.3 ± 4.2	L-C
7	Xerocrept	1570 ± 70	7.2 ± 0.10	0.60 ± 0.24	6.7 ± 0.3	2.5 ± 0.3	S
8	Ustalfs (ferrallitic)	1001	5.0	3.23	54.8 ± 4.6	46.0 ± 3.9	C

† ρ_b , bulk density; OM, organic matter; θ_{33} and θ_{1500} , soil water content at 33 and 1500 kPa, respectively; texture symbols (USDA): clay (C), sand (S), and loam (L).

$$\frac{d\tau}{d\rho} = \frac{3\rho(\rho - 1)}{a^3 - \rho^3} \quad [4]$$

in terms of the dimensionless variables τ and ρ

$$\tau = \frac{8K_s t}{\pi^2 r_o^2}; \quad \rho = \frac{R}{r_o}; \quad a^3 = \frac{3(\Psi + h_o + \pi^2 r_o^2 / 8)}{r_o \Delta\theta} + 1 \quad [5]$$

and subject to the boundary condition $\tau = 0$ ($\rho = 1$). Integrating Eq. [4] we obtain an expression that relates both the nondimensional time (τ) and water level in the pipe (ρ) as a function of the Green–Ampt's wetting front suction, Ψ , and the increment in soil water content ($\Delta\theta$) after an experiment:

$$\tau(\Delta\theta, \Psi) = \left(1 + \frac{1}{2a}\right) \log\left(\frac{a^3 - 1}{a^3 - \rho^3}\right) - \frac{3}{2a} \log\left(\frac{a - 1}{a - \rho}\right) + \frac{\sqrt{3}}{a} \arctan\left(\frac{\sqrt{3}a(\rho - 1)}{2a^2 + a(\rho + 1) + 2\rho}\right) \quad [6]$$

Several methods have been proposed to estimate K_s and Ψ from Eq. [6]. Philip (1993) computed K_s and Ψ from the plots t_{\max}/t_{med} vs. τ_{\max} and t_{\max}/t_{med} vs. Ψ . By contrast De Haro et al. (1998) proposed finding the global minimum of the objective function $\tau_{\max}/\tau_{\text{med}} - t_{\max}/t_{\text{med}} = 0$, subjected to the following constraints:

$$\text{Upper bound: } a > \rho_{\max} \quad [7a]$$

$$\text{Lower bound: } \lim_{a \rightarrow \infty} \frac{\tau_{\max}}{\tau_{\text{med}}} = \frac{1 - 3\rho_{\max}^2 + 2\rho_{\max}^3}{1 - 3\rho_{\text{med}}^2 + 2\rho_{\text{med}}^3} \quad [7b]$$

Muñoz-Carpena et al. (2002) compared the De Haro et al. (1998) method with two alternatives. One solves the two-dimensional system $t_{\max} = t_{\max}(K_s, \Psi)$; $t_{\text{med}} = t_{\text{med}}(K_s, \Psi)$, and this is compared with the nonlinear fitting of $\tau = \tau(\rho)$ to the experimental data set (t_i, h_i), yielding consistent results. In either case the estimation of K_s and Ψ is numerically demanding, and thus such methods have developed ad hoc numerical codes (Muñoz-Carpena and Álvarez-Benedí, 2002).

PHILIP–DUNNE MEASUREMENTS

The infiltration data studied come from previous work performed in soils with a wide range of textural and physicochemical properties (Tables 1 and 2). We consider in this study the measurements ($n = 70$) from Muñoz-Carpena et al. (2002) in an andic agricultural

soil (Soil 1); the measurements performed by García-Sinovas et al. (2001) in three experimental plots (Soils 2–4) in Valladolid, Spain with different soil textures (Antolín Barriuso, 2001); later experiments in a Valladolid plot with a $n = 100$ sample data size (Soil 5) (García-Sinovas et al., 2002); and measurements ($n = 57$) performed with the Philip–Dunne permeameter in a organic forest soil (Soil 6) in the Garajonay National Park, La Gomera (Regalado, 2003). To broaden the spectrum of textural classes investigated measurements of hydraulic properties of a sandy soil (97.7% sand, Soil 7) and a clay soil (83.5% clay, Soil 8) were also performed. The clayey horizon was described in Fernández-Caldas et al. (1982). Thus, 308 samples from eight different soils were analyzed, so the conclusions presented are considered sufficiently general to be extrapolated to other scenarios. The analysis presented here is also supported by general theoretical results independent of the soil characteristics, reinforcing its applicability. The Philip–Dunne permeameter design and measurement protocol used in all soils of this study were described by Muñoz-Carpena et al. (2002); $r_i = 0.018$ m and $h_o = 0.3$ m.

RESULTS AND DISCUSSION

Estimation of K_s and S

The limitation of Philip's method to compute K_s and S from measurements of t_{med} , t_{\max} , and $\Delta\theta$ is closely related to the problem of obtaining a relatively large (García-Sinovas et al., 2001) or small (Muñoz-Carpena et al., 2002) number of K_s values outside the upper (Eq. [7a]) and lower (Eq. [7b]) bounds. Something similar happens with the negative K_s values obtained with the constant-head well permeameter method that previous authors have explained in terms of soil heterogeneity

Table 2. K_s , Ψ , and S values (geometric mean ± standard deviation) obtained with the Philip–Dunne permeameter for soil samples used in this study (n : number of measurements).

Soil	n	K_s		Ψ		S	
		m s ⁻¹		m		m s ^{-1/2}	
1	70	7.43 ± 4.99 × 10 ⁻⁵	1.25 ± 3.52 × 10 ⁻²	5.13 ± 2.45 × 10 ⁻⁴			
2	40	1.59 ± 2.06 × 10 ⁻⁵	1.02 ± 9.64 × 10 ⁻²	2.67 ± 9.59 × 10 ⁻⁴			
3	11	1.25 ± 3.66 × 10 ⁻⁵	9.74 ± 4.85 × 10 ⁻³	1.56 ± 6.89 × 10 ⁻⁴			
4	10	1.36 ± 9.55 × 10 ⁻⁴	2.83 ± 9.91 × 10 ⁻²	1.38 ± 5.48 × 10 ⁻³			
5	100	3.37 ± 6.10 × 10 ⁻⁵	2.48 ± 9.37 × 10 ⁻²	4.85 ± 4.95 × 10 ⁻⁴			
6	57	4.16 ± 6.95 × 10 ⁻⁵	1.06 ± 5.04 × 10 ⁻²	4.32 ± 5.33 × 10 ⁻⁴			
7	10	9.56 ± 3.14 × 10 ⁻⁴	1.85 ± 0.80 × 10 ⁻²	2.46 ± 0.30 × 10 ⁻³			
8	10	2.39 ± 3.14 × 10 ⁻⁶	8.81 ± 5.85 × 10 ⁻²	1.48 ± 0.74 × 10 ⁻⁴			

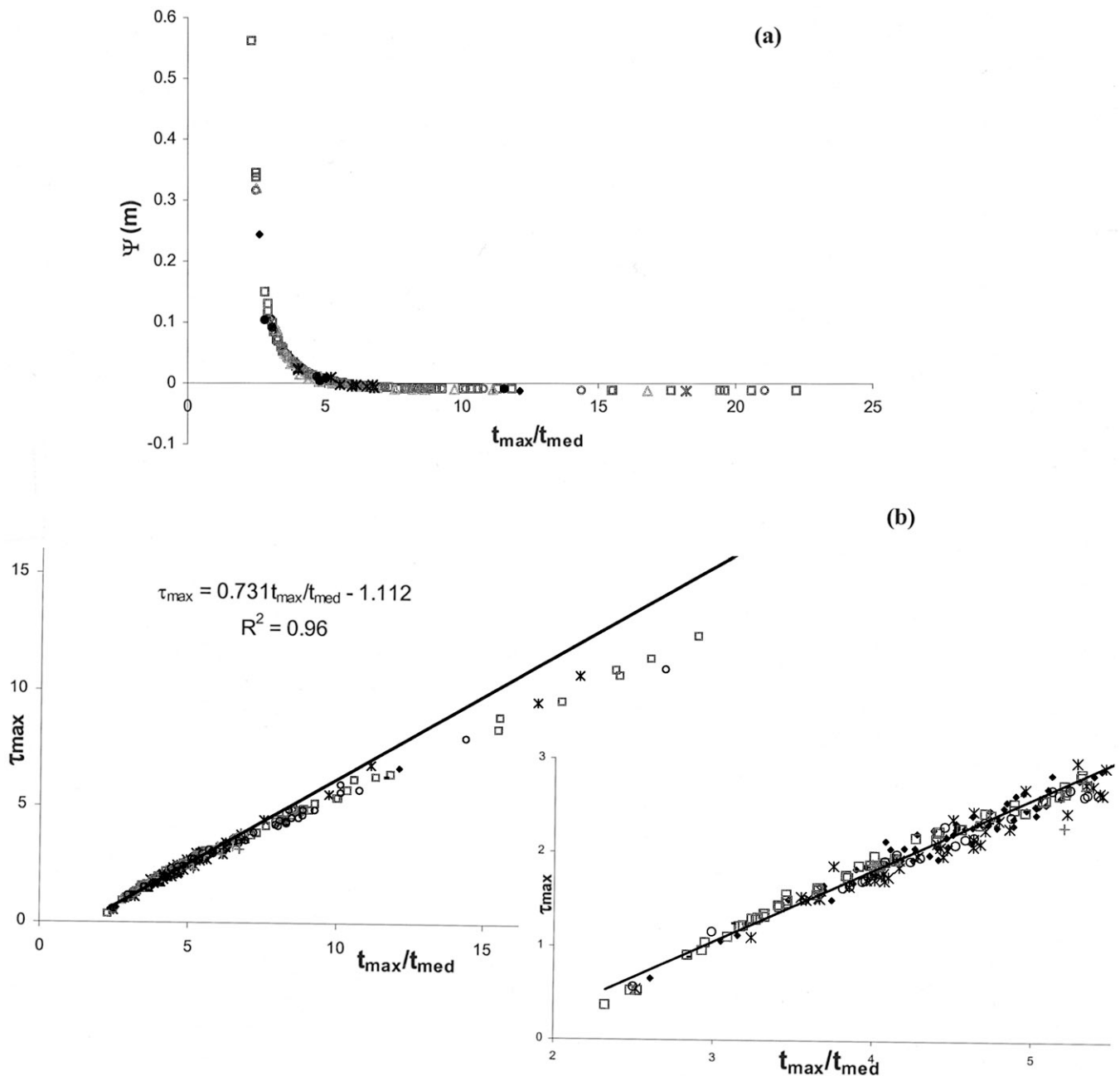


Fig. 2. (a) t_{\max}/t_{med} vs. Ψ , and (b) t_{\max}/t_{med} vs. τ_{\max} relationships for the 308 measurements performed in eight different soils (represented by different symbols). Insert in (b) represents t_{\max}/t_{med} vs. τ_{\max} values where Ψ is positive.

(Elrick and Reynolds, 1992). In the constant-head well permeameter method this has been “solved” by the one-head approach (with the limitations described above) or a regression-based approach, which makes use of the constraints $K_s > 0$ and $\Psi > 0$ to recompute the negative conductivity and wetting front suction values (Reynolds et al., 1992). With the Philip–Dunne method, no methods have been developed to solve this problem, apart from the relaxation of the constraint (Eq. [7a]) $a > \rho_{\max}$, but this implies $\Psi < 0$, which is not physically valid. Negative Ψ values, and consequently invalid measurements of K_s and S , may arise because of sensitivities and ill-posedness resulting from the Green–Ampt model and simplifying assumptions (rigid, homogeneous, iso-

tropic soil with uniform initial water content) incorporated into Philip’s analysis. If the soil has heterogeneities, such as macropores, layering, or preferential flow zones, the wetted bulb will likely have an irregular shape. This also may be the case for a clay soil where mineral particles are anisotropically oriented, and therefore the hydraulic conductivity may be larger in the horizontal than in the vertical direction. We would then expect an oblate spheroidal bulb. The presence of preferential vertical flow paths or stones would facilitate the gravitational flow of water, and this would lead to a vertically elongated bulb. In both situations the wetted bulb eccentricity, ecc , ($-1 < \text{ecc} < 1$) departs from the null value, $\text{ecc} = 0$, of a sphere. In such situations Philip’s analysis,

developed for the spherical case, becomes limited and would need to be modified by considering the wetted bulb's eccentricity.

Following the method of Philip (1993) to estimate K_s and Ψ from observations of $h(t)$, Fig. 2 represents the relation t_{\max}/t_{med} vs. Ψ and t_{\max}/t_{med} vs. τ_{\max} for the total 308 samples of the eight soils studied. Two conclusions may be drawn. First it can be noticed that for $t_{\max}/t_{\text{med}} > 5.4$ the suction at the wetting front violates the positivity condition (Fig. 2a). The value $t_{\max}/t_{\text{med}} \approx 5.4$ also sets the limit where $(t_{\max}/t_{\text{med}}, \tau_{\max})$ diverges from the line ($r^2 = 0.96$):

$$\tau_{\max} = 0.731 \frac{t_{\max}}{t_{\text{med}}} - 1.112, \quad t_{\max}/t_{\text{med}} < 5.4 \quad [8]$$

obtained from the data points that satisfy $\Psi > 0$ (insert in Fig. 2b). A general analytical expression of the crossing point $t_{\max}/t_{\text{med}} \approx 5.4$ may be obtained by setting $\Psi = 0$ in Eq. [6] such that this value of $t_{\max}/t_{\text{med}} \approx 5.4$ is thus related to the permeameter's dimensions r_i and h_o . Since K_s and Ψ are coupled through Eq. [6], the t_{\max}/t_{med} values corresponding to $\Psi < 0$ are not valid for computing the corresponding τ_{\max} and must thus be discarded.

The fitting line (Eq. [8]) is obtained from soils with different characteristics and antecedent water content. Hence, given the values of t_{med} and t_{\max} , this provides a rapid and simple method to compute τ_{\max} , and therefore K_s from $\tau_{\max} = 8K_s t_{\max}/(\pi^2 r_o)$. Notice that at least in principle τ depends not only on K_s and Ψ , but also on $\Delta\theta$, as can be deduced from Eq. [6]. However, the generality of the fitting curve obtained seems to contradict this assertion. This independence of τ on $\Delta\theta$ is only so in appearance and indicates the small weight of $\Delta\theta$ in Eq. [6], as we demonstrate subsequently by a sensitivity analysis.

A reasonable fitting ($r^2 = 0.98$) of the points $(t_{\max}/t_{\text{med}}, \Psi)$ shown in Fig. 2a is obtained with a simple model with only two parameters:

$$\log \Psi = a' + b' \sqrt{\frac{t_{\text{med}}}{t_{\max}}} \quad [9]$$

where $a' = -13.503$ and $b' = 19.678$, and $0.01 \text{ m} < \Psi < 1 \text{ m}$. Equation [9] implies that a semi-log plot of Ψ vs. $(t_{\text{med}}/t_{\max})^{1/2}$ will easily help to detect outliers. The goodness of fit of both derived equations (Eq. [8] and [9]) is evaluated by comparing these with the solution obtained by solving numerically the full system (Eq. [6]) and evaluating the coefficient of determination of the 1:1 line (Fig. 3). The r^2 of the 1:1 line is high in all cases (K_s , Ψ , and S) and thus we may consider the above simplified method, which is independent of $\Delta\theta$, satisfactory.

As we have already discussed, it is interesting that despite the dependence of τ on $\Delta\theta$, as given by Eq. [6], we can obtain a fitting curve (Eq. [9]) that is independent of the soil moisture increment for a wide range of soils. This dependence of t on $\Delta\theta$ is studied next, making use of Eq. [6]. Figure 4 shows the superposition of the data pairs $(t_{\max}/t_{\text{med}}, \Psi > 0)$ with the analytical curve $t_{\max}/t_{\text{med}} = f(\Delta\theta, \Psi)$ obtained from Eq. [6] for two extremely different water content increments: $\Delta\theta = 0.05$ and 0.5

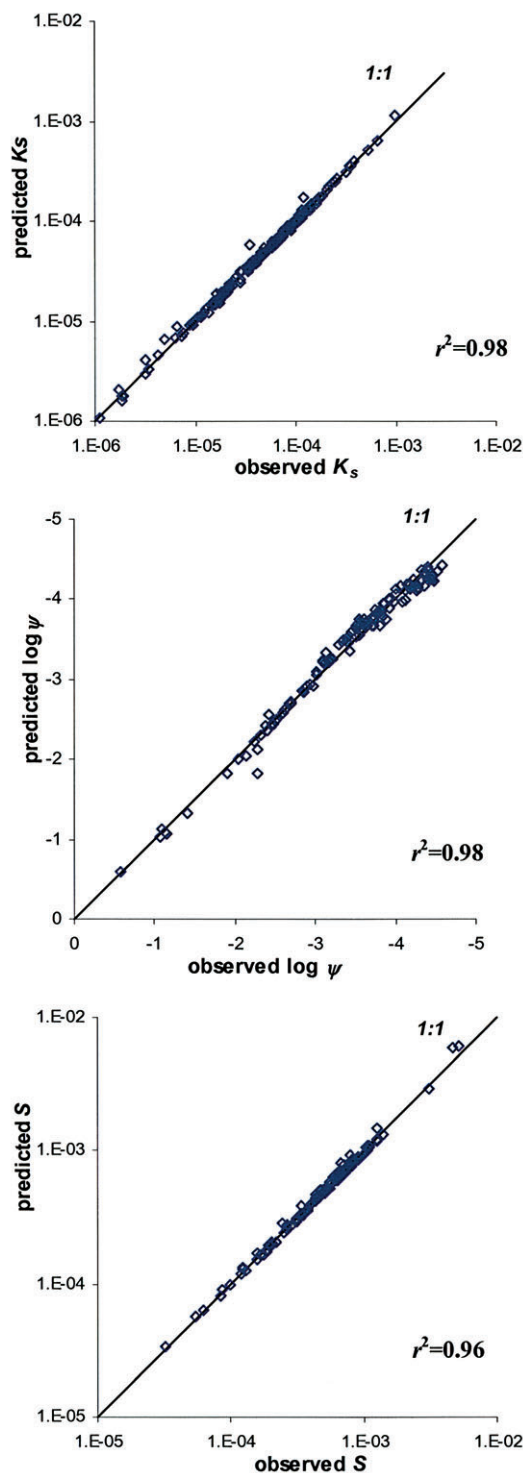


Fig. 3. Goodness of fit of both derived equations (Eq. [8] and [9]) to compute K_s , Ψ , and S evaluated by comparing these with the solution obtained by solving numerically the full system (Eq. [6]).

$\text{m}^3 \text{ m}^{-3}$. As can be observed in Fig. 4, an increase of one order of magnitude in $\Delta\theta$ implies a small modification in the shape of the curve, and this explains the weak dependence of $t_{\max}/t_{\text{med}} = f(\Delta\theta, \Psi)$ on $\Delta\theta$, and consequently why it is possible to represent this by a unique fitting curve independent of $\Delta\theta$. In fact the Green-Ampt's wetting front suction parameter can be estimated from

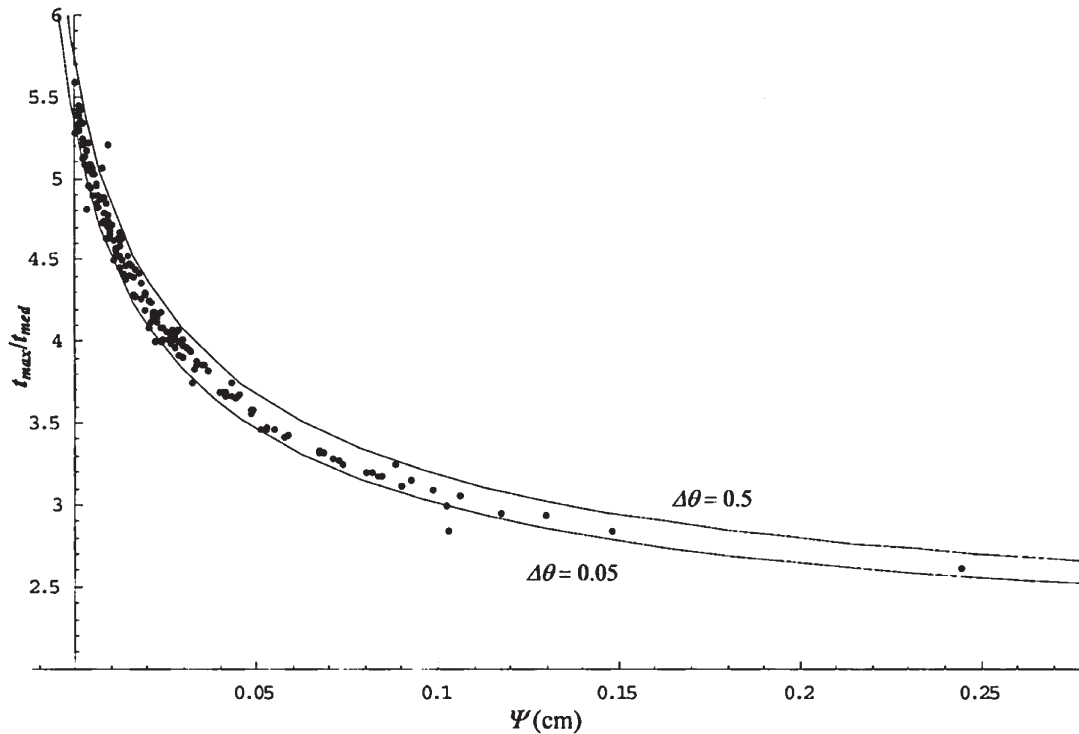


Fig. 4. Plot of the data pairs $(t_{\max}/t_{\text{med}}, \Psi > 0)$ and the curve $t_{\max}/t_{\text{med}} = f(\Delta\theta, \Psi)$ obtained from Eq. [6] for two different water content increments: $\Delta\theta = 0.05 \text{ m}^3 \text{ m}^{-3}$ (lower curve) and $\Delta\theta = 0.5 \text{ m}^3 \text{ m}^{-3}$ (upper curve). Notice that the axes are inverted with respect to Fig. 2.

the soil's pore size-distribution (Rawls and Brakensiek, 1983), independently of the soil water content, as will be discussed in the next section.

Sensitivity Analysis

From the point of view of the Philip–Dunne permeameter field applicability, a sensitivity analysis would help us establish the precision required for the measured time course of water depth and soil moisture increments. From the above discussion it is clear that the relation t_{\max}/t_{med} plays an important role in the behavior of K_s and Ψ , and hence the sorptivity $S \approx (2K_s\Psi\Delta\theta)^{1/2}$. This is why the relation t_{\max}/t_{med} is used next as a varying parameter in the sensitivity analysis. Previous authors did not consider the effect of variations in the ratio t_{\max}/t_{med} in their K_s sensitivity analysis (De Haro et al., 1998). Figure 5 shows the K_s , Ψ , and S sensitivity coefficients, SC (percentage of variation with respect to the initial value) for different initial ratios $t_{\max}/t_{\text{med}} = 2.61, 3.74,$ and 5.38 , changing h_0 , t_{\max} , t_{med} , and $\Delta\theta$ in $\pm 1\%$ steps, within the interval $[-20\%, 20\%]$, around the mean value. Initial values of h_0 and $\Delta\theta$ are, respectively, 0.3 m and $0.26 \text{ m}^3 \text{ m}^{-3}$. For the sensitivity analysis, Eq. [6] is used, and the values of K_s and Ψ are thus found numerically as described in Muñoz-Carpena et al. (2002). Notice that the selected ratios t_{\max}/t_{med} are representative of K_s and Ψ values either far from or close to the region where Ψ becomes negative (see Fig. 2). These time ratios correspond to initial K_s and Ψ values of $2.19 \times 10^{-5} \text{ m s}^{-1}$, $27.20 \times 10^{-3} \text{ m}$ ($t_{\max}/t_{\text{med}} = 2.61$); $5.91 \times 10^{-5} \text{ m s}^{-1}$, $4.09 \times 10^{-3} \text{ m}$ ($t_{\max}/t_{\text{med}} = 3.74$); and $1.00 \times 10^{-4} \text{ m s}^{-1}$, $1.61 \times 10^{-4} \text{ m}$ ($t_{\max}/t_{\text{med}} = 5.38$). We also investigate the effect that

variations in the geometric coefficient, g_c , have on the sensitivity of K_s , Ψ , and S . This g_c factor is used by Philip (1993) to adjust the model's spherical flow to the actual flow paths and it is set to an approximate value of $8/\pi^2$ (Fig. 1). The sensitivity analysis of g_c will allow us to study the sensitivity of Philip's model to this hypothesis. As mentioned above, OX axes in Fig. 5 indicate the percentage of parameter variation, while OY axes show the corresponding SC expressed in terms of percentage of deviation from the initial value (for K_s , Ψ , and S). Several conclusions may be obtained from the sensitivity analysis shown in Fig. 5:

1. The maximum (t_{\max}) and medium (t_{med}) drawdown times are the parameters that most affect the estimated K_s , Ψ , and S values. Errors made in the readings of t_{\max} and t_{med} partially compensate each other, since the slope of the t_{\max} and t_{med} sensitivity curves have opposite signs (see also De Haro et al., 1998).
2. The slopes of the t_{\max} and t_{med} sensitivity curves have different signs in the case of Ψ and S , compared with that of K_s .
3. The sensitivity of Ψ to t_{\max} and t_{med} is greater than the sensitivity of K_s and S to such drawdown times, especially for low and medium t_{\max}/t_{med} ratios.
4. The sensitivity to $\Delta\theta$ is in all instances relatively small compared with that of the other parameters. This agrees with the previous discussion about Fig. 4.
5. The sensitivity to the permeameter's height (h_0) and the g_c coefficient is small. However, this is relatively high for Ψ and S (but not so for K_s) for the ratio $t_{\max}/t_{\text{med}} = 5.38$, close to the point where Ψ

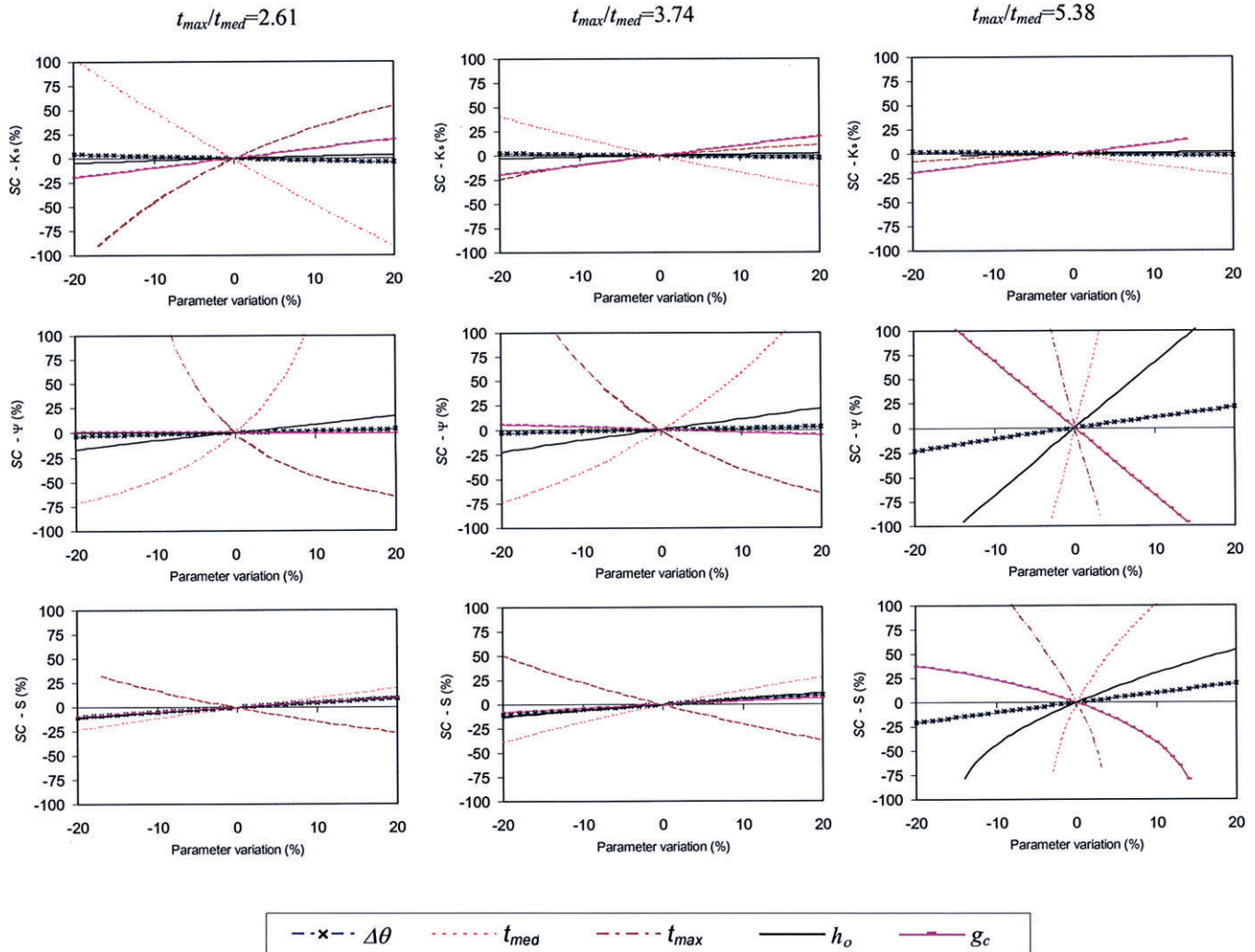


Fig. 5. Sensitivity analysis of K_s , Ψ , and S (OY axes) to variations of parameters: h_0 , t_{max} , t_{med} , $\Delta\theta$, and g_c (represented by different line types) within the interval $[-20\%, 20\%]$, for various initial ratios $t_{max}/t_{med} = 2.61, 3.74,$ and 5.38 (from left to right). In those cases where the parameter combination yielded $\Psi < 0$, the solving algorithm ceases to compute and thereby no SC was calculated. The sensitivity coefficient, SC, represents the percentage of variation with respect to the initial value (OY axes).

becomes negative. Such a g_c coefficient was approximately set to $8/\pi^2$ (≈ 0.8) by Philip (1993) to match the flow through the actual system with that of the approximated spherically symmetrical (Fig. 1). The current analysis suggests that the model may be rather sensitive to such a geometrical hypothesis for large t_{max}/t_{med} ratios.

6. Finally, the sensitivity of Ψ and S , but not of K_s , to all parameters investigated (with the exception of $\Delta\theta$) increases drastically as t_{max}/t_{med} becomes larger, such that close to $t_{max}/t_{med} \approx 5.4$, Ψ and S become very sensitive to small variations ($<2\%$) in t_{max} , t_{med} , h_0 , and g_c .

The sensitivity analysis just shown depends on the initial or standard values of the implied variables. We further investigated how the above conclusions may be modified when assuming different initial values of the soil water content increment, $\Delta\theta$: 0.10, 0.26 (already shown in Fig. 5), and $0.35 \text{ m}^3 \text{ m}^{-3}$. The sensitivity curves were unaltered for initial $t_{max}/t_{med} = 2.61$ and 3.74 (results

not shown); thus, the above conclusions may be considered general and independent of the initial value of $\Delta\theta$. However for initial $t_{max}/t_{med} = 5.38$, the sensitivity scenario changes (Fig. 6).

For initial $t_{max}/t_{med} = 5.38$, the K_s sensitivity curves remained unaltered by choosing different initial $\Delta\theta$ (see the first row in Fig. 6). By contrast the Ψ and sorptivity curves change significantly as the initial $\Delta\theta$ decreases. The same sensitivity trend is maintained as $\Delta\theta$ diminishes, but the sensitivity coefficients increase drastically with parameter variation (second and third row in Fig. 6). Visually, we can depict this as if the sensitivity curves were pulled out from their extremes as the initial $\Delta\theta$ increases. Notice that for $\Delta\theta = 0.1 \text{ m}^3 \text{ m}^{-3}$, the sensitivity to some of the parameters is so high that errors of $<5\%$ in, for example, the drawdown times t_{max} and t_{med} can lead to estimate errors in Ψ of one order of magnitude (1000% in SC- Ψ). These conditions, however, correspond to a low Green–Ampt wetting front suction ($\Psi = 2.4 \times 10^{-5} \text{ m}$) and therefore to predominance of gravitational

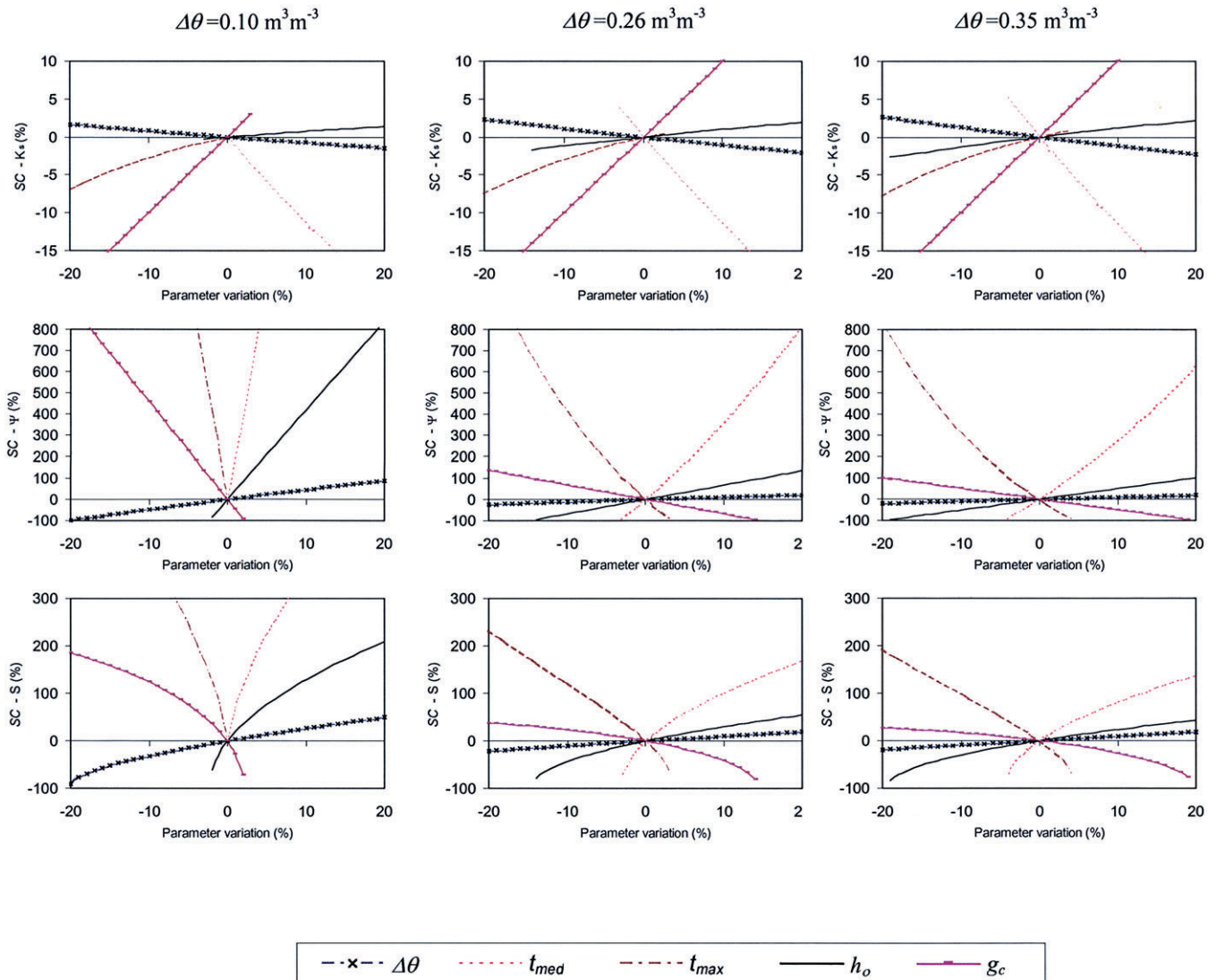


Fig. 6. Sensitivity analysis of K_s , Ψ , and S (OY axes) to variations of parameters: h_o , t_{max} , t_{med} , $\Delta\theta$, and g_c (represented by different line types) within the interval $[-20\%, 20\%]$, for an initial ratio $t_{max}/t_{med} = 5.38$ with different initial values of $\Delta\theta = 0.10, 0.26,$ and $0.35 \text{ m}^3 \text{ m}^{-3}$ (from left to right). In those cases where the parameter combination yielded $\Psi < 0$, the solving algorithm ceases to compute and thereby no SC was calculated. The sensitivity coefficient, SC, represents percentage of variation with respect to the initial value (OY axes).

forces over pressure-capillarity (see Section 7 in Philip, 1993). As mentioned above, Philip’s analysis considers that water flow out of the permeameter is primarily driven by pressure-capillarity and that this is perturbed by superposing on it the gravitational component. Under conditions of very low wetting front suction, as the one considered above, such an assumption no longer holds, and therefore results must be taken with care. From Philip (1993) the ratio of the capillary to gravitational components of the flow, $\Omega = 8\Psi/\pi^2 r_o$, provides the following “safety” limit of $\Psi > 0.011 \text{ m}$ (with $r_o = 0.009 \text{ m}$) for this assumption to be satisfied (i.e., $\Omega > 3.11$).

CONCLUSIONS

The sorptivity may provide information about relevant hydraulic and structural soil properties, such as the soil diffusivity, the unsaturated hydraulic conductivity curve, and the macroscopic capillary length parameter,

α^* . The Philip–Dunne falling-head permeameter can estimate the field sorptivity from $S \approx (2K_s\Psi\Delta\theta)^{1/2}$. We have shown that the ratio t_{max}/t_{med} governs the behavior of both K_s and Ψ . The following system of equations:

$$\tau_{max} = 0.731 t_{max}/t_{med} - 1.112, \quad t_{max}/t_{med} < 5.4 \quad [10a]$$

$$\tau_{max} = 8K_s t_{max}/(\pi^2 r_o) \quad [10b]$$

$$\log\Psi = -13.503 + 19.678(t_{max}/t_{med})^{-1/2}, \quad 0.01 \text{ m} < \Psi < 1 \text{ m} \quad [10c]$$

renders the values of K_s and Ψ by measuring only the t_{max}/t_{med} ratio. This method turns out to be more convenient than previous numerical routines, particularly in field conditions, where the use of a handheld calculator or portable PC may not be feasible. Furthermore, it is not necessary to measure $\Delta\theta$, a relatively costly determination, to be able to estimate K_s and Ψ . The fitting curves obtained are sufficiently general as to avoid the

need for such numerical algorithms, since the K_s and Ψ values obtained by Philip's method (already approximate) may be considered at their best an estimation of the order of magnitude of such soil properties (as it has been previously shown by comparisons with other permeameters). As a rule of thumb, the relation $t_{\max}/t_{\text{med}} < 5$ allows us to quickly discard invalid field experiments that would have to be repeated until an appropriate time ratio is obtained. Furthermore, the high sensitivity of the soil sorptivity and wetting front suction estimates near $t_{\max}/t_{\text{med}} \approx 5.4$ suggests that drawdown time measurements and water depths must be done with great precision. All this reinforces the idea of an automatic reading of t_{\max} , t_{med} , and h_0 , something that has been already explored by previous authors (Alvarez-Benedí et al., 2003), if the Philip–Dunne falling-head permeameter is to be considered a valid alternative to other field methods for measuring the soil sorptivity. The current work stresses that the Philip–Dunne falling head permeameter is a low cost technique, especially useful for low conductivity soils and where personnel and resources are limited.

ACKNOWLEDGMENTS

This work has been supported with funds from INIA-Plan Nacional de I+D Agrario (Project numbers SC99-024-C2 and RTA-01-097). The authors would like to thank D. García Sinovas at Instituto Tecnológico Agrario (Valladolid) for the experiments carried out in the Valladolid plots, J.V. Giráldez from University of Córdoba for his helpful comments, and D. Fernández for the drawings in Fig. 1. This research was supported by the Florida Agricultural Experiment Station, and approved for publication as Journal Series no. R-10139.

REFERENCES

- Alvarez-Benedí, J., D. García-Sinovas, and R. Muñoz-Carpena. 2003. Determinación de la conductividad hidráulica en suelos mediante un permeámetro de carga variable automatizado. *Innovación* 15:7–16.
- Antolín Barriuso, R. 2001. Caracterización espacial de la conductividad hidráulica en parcelas experimentales mediante los permeámetros de Guelph y Philip–Dunne. Trabajo Fin de Carrera. Escuela Técnica Superior de Ingenierías Agrarias, Palencia, Spain.
- Brutsaert, W. 1979. Universal constants for scaling the exponential soil water diffusivity? *Water Resour. Res.* 15:481–483.
- De Haro, J.M., K. Vanderlinden, J.A. Gómez, and J.V. Giráldez. 1998. Medida de la conductividad hidráulica saturada. p. 9–20. *In* A. González et al. (ed.). *Progresos en la Investigación de la Zona No Saturada*. *Collectanea*, 11. Available at www.zonanosaturada.com/jornadas/jornadas.htm (verified 14 Feb. 2005). Universidad de Huelva, Huelva, Spain.
- Elrick, D.E., and W.D. Reynolds. 1992. Infiltration from constant-head well permeameters and infiltrometers. p. 1–24. *In* G.C. Topp et al. (ed.). *Advances in measurements of soil physical properties: Bringing theory into practice*. SSSA Spec. Publ. 30. SSSA, Madison, WI.
- Fernández-Caldas, E., M.L. Tejedor-Salguero, and P. Quantín. 1982. Suelos de regiones volcánicas. Tenerife, Islas Canarias. Colección Viera y Clavijo IV. Secretariado de publicaciones de la Universidad de La Laguna, CSIC, La Laguna, Spain.
- García-Sinovas, D., M.A. Andrade-Benítez, C.M. Regalado-Regalado, and J. Álvarez-Benedí. 2002. Variabilidad espacial de la conductividad hidráulica medida con el permeámetro de Philip–Dunne. p. 53–57. *In* J. Dafonte et al. (ed.). *Resúmenes de las I Jornadas sobre Agricultura de Precisión*. A Coruña, Spain.
- García-Sinovas, D., C.M. Regalado, R. Muñoz-Carpena, and J. Álvarez-Benedí. 2001. Comparación de los permeámetros de Guelph y Philip–Dunne para la estimación de la conductividad hidráulica saturada del suelo. p. 31–36. *In* J.J. López Rodríguez and M. Quemada Sáenz-Badillos (ed.). *Temas de Investigación en Zona no saturada*. Available at www.zonanosaturada.com/jornadas/jornadas.htm (verified 14 Feb. 2005). Universidad Pública de Navarra, Navarra, Spain.
- Gardner, W.R. 1958. Some steady-state solutions of the unsaturated moisture flow equation with application to evaporation from a water table. *Soil Sci.* 85:3228–3232.
- Gómez, J.A., J.V. Giráldez, and E. Fereres. 2001. Analysis of infiltration and runoff in an olive orchard under no-till. *Soil Sci. Soc. Am. J.* 65:291–299.
- Minasny, B., and A.B. McBratney. 2000. Estimation of sorptivity from disc-permeameter measurements. *Geoderma* 95:305–324.
- Muñoz-Carpena, R., and J. Álvarez-Benedí. 2002. WPDUNNE Ver. 1.0. Available at <http://carpena.ifas.ufl.edu> (verified 14 Feb. 2005). UF-ITACL, Gainesville, FL and Valladolid, Spain.
- Muñoz-Carpena, R., C.M. Regalado, J. Álvarez-Benedí, and F. Bartoli. 2002. Field evaluation of the new Philip–Dunne permeameter for measuring saturated hydraulic conductivity. *Soil Sci.* 167:9–24.
- Philip, J.R. 1969. Theory of infiltration. *Adv. Hydrosci.* 5:215–296.
- Philip, J.R. 1985. Approximate analysis of the borehole permeameter in unsaturated soil. *Water Resour. Res.* 21:1025–1033.
- Philip, J.R. 1987. The infiltration joining problem. *Water Resour. Res.* 23:2239–2245.
- Philip, J.R. 1993. Approximate analysis of falling-head lined borehole permeameter. *Water Resour. Res.* 29:3763–3768.
- Rawls, W.J., and D.L. Brakensiek. 1983. A procedure to predict Green Ampt infiltration parameters. p. 102–112. *In* *Advances in infiltration*, Proc. Natl. Conf. on Advances in Infiltration, Chicago, IL. 12–13 Dec. 1983. ASAE, St. Joseph, MI.
- Regalado, C.M. 2003. Ajuste del balance hidrológico y simulación por ordenador del comportamiento de una cuenca forestal de laurisilva en el Parque Nacional de Garajonay. INIA-RTA-01-097 Project rep. INIA, Madrid.
- Reynolds, W.D., S.R. Vieira, and G.C. Topp. 1992. An assessment of the single-head analysis for the constant head well permeameter. *Can. J. Soil Sci.* 72:489–501.
- White, I., and M.J. Sully. 1987. Macroscopic and microscopic capillary length and time scales from field infiltration. *Water Resour. Res.* 23:1514–1522.
- Youngs, E.G. 1964. An infiltration method measuring the hydraulic conductivity of unsaturated porous materials. *Soil Sci.* 97:307–311.